Analytic design and solutions for resonance domain diffractive optical elements

Michael A. Golub

Department of Physical Electronics, Faculty of Engineering, Tel Aviv University, Ramat Aviv 69978, Israel

Asher A. Friesem

Department of Physics of Complex Systems, Weizmann Institute of Science, Rehovot 76100, Israel

Received July 5, 2006; revised September 25, 2006; accepted September 26, 2006;
posted October 2, 2006 (Doc. ID 72721); published February 14, 2007

A model for designing and analyzing complicated surface relief diffractive elements in the resonance domain is developed. It is based on subdividing the complicated diffractive element into many highly efficient local diffraction gratings whose surface relief modulations can be effectively characterized as slanted volume gratings for which closed form analytic solutions exist. The model is illustrated by finding in the resonance domain the local period, effective slant angle, and groove depth at each location on an off-axis cylindrical diffractive lens.

OCIS codes: 050.1970, 050.1950, 260.1960, 260.2110, 050.2770, 050.1380.

1. INTRODUCTION

Diffractive optical elements (DOEs) are usually designed and characterized with scalar diffraction Fourier methods[1] and scalar analytical ray tracing for beam focusing and shaping.[2–4] The scalar analytical ray tracing is based on first-order beam diffraction at each point of the DOE, similar to refraction at each point of a conventional refractive optical element. Accordingly, a local diffraction grating approximation, where light is diffracted by the angles defined by a local spatial frequency and the grating period on the DOE, is exploited. The scalar diffraction designs where the DOE grating period is significantly larger (at least ten times) than the illumination wavelength have advanced to the level at which either analytical equations or well-defined iterative algorithms have been established and successfully applied.

Unfortunately, when the local grating period of the DOEs is comparable to the illumination wavelength in the resonance domain of diffraction, the situation is much more complex. Typically, numerical methods of rigorous diffraction theory[5–9] are exploited for designing such DOEs whose local diffraction gratings have high diffraction angles.[10–16] When the grating period is smaller than the illumination wavelength, namely, in the subwavelength domain, there are well-developed analytical models of effective medium theory. They are based on substitution of grating grooves by an averaged effective medium layer.[17]

In this paper we present a method that combines the simplicity of the scalar diffraction design with the accuracy of rigorous diffraction for designing DOEs with surface relief gratings. This method is applied to DOEs that obey two conditions. First, they are in the resonance domain. Second, their first-order diffracted beam is restricted by geometrical optics and, consequently, the DOE may be treated as built-up from local surface relief diffraction gratings with gradually variable grating orientation and groove parameters. The local diffraction grating should be designed to transform the angular orientation of the local incident beam to that of the local diffracted beam with high diffraction efficiency. Diffraction efficiency and phase are estimated with an analytical effective grating model that is based on the Bragg properties of the local surface relief gratings.[18–21] We show that the parameters of the local grating grooves (period, depth, effective slant angle, orientation shape) may be chosen with a simple set of analytical equations. Computer simulations of specific diffraction gratings and off-axis diffractive elements confirm the validity and applicability of our method.

2. HIGHLY EFFICIENT DIFFRACTIVE OPTICAL ELEMENTS

The approach we propose for the DOE is quite similar to that for kinoform diffractive elements[1] in terms of input to output beam transformation, but exploits resonance domain diffraction[18] rather than classical scalar diffraction. We consider a basic DOE, recorded either holographically or by direct writing process, on planar or curved substrates. The relevant parameters and geometry of the DOE and beam transformation are depicted in Fig. 1, where h is the maximum height of the grating grooves; Λ the grating period; n_M the refractive index of the groove material; n_i the refractive index of the surrounding medium (normally air so $n_i=1$); θ_{inc}, $\mathbf{N}_{inc}$, and S_{inc} characterize the local angular orientation and phase distribution (eikonal) of the incident beam; θ_{out}, $\mathbf{N}_{out}$ and S_{out} characterize the local angular orientation and phase distribution (eikonal) of the output diffracted beam; $\mathbf{N}_n$ is the local unit normal to the DOE substrate and pointing to the side of beam propagation; and $\mathbf{x}$ the lateral coordinate

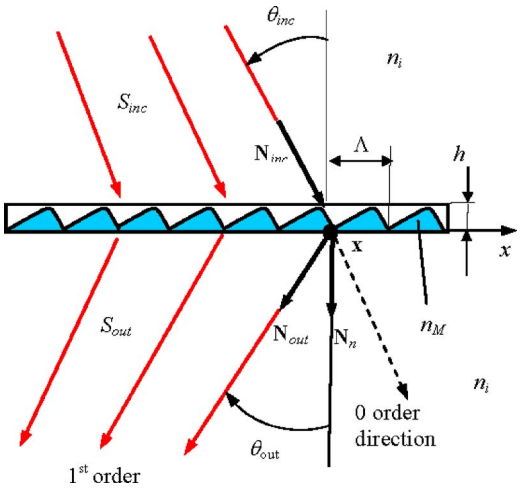

Fig. 1. (Color online) Relevant parameters and geometry of a beam-transforming DOE.

along the DOE surface. Obviously, angles and unit ray vectors of the incident and output diffracted beams are related as

$$\cos\theta_{inc} = \mathbf{N}_{inc}\cdot\mathbf{N}_n, \quad \cos\theta_{out} = \mathbf{N}_{out}\cdot\mathbf{N}_n. \tag{1}$$

We assume that the DOE is illuminated with a monochromatic beam that obeys the restrictions of geometrical optics and has a wavelength λ and eikonal function S_{inc}. In accordance with the eikonal equation of geometrical optics, the unit ray vector $\mathbf{N}_{inc}$ is

$$\mathbf{N}_{inc} = \frac{\nabla S_{inc}}{n_i}, \tag{2}$$

where ∇ is the 3-D gradient operator.

We now assume that the incident power is diffracted, with $\approx$100% diffraction efficiency, only into the first diffraction order, which constitutes the output beam. This output beam is characterized by the eikonal S_{out} and can be, in general, either a simple spherical wave or a more complex aspherical wave needed for imaging or laser beam shaping and focusing. Several classes of diffractive elements, like diffractive lenses[2] and map-transformation beam shapers,[3] have closed form analytical equations for S_{out}. When S_{out} satisfies geometrical optics restrictions, then the local direction $\mathbf{N}_{out}$ of the output beam is determined with the aid of the eikonal equation of geometrical optics

$$\mathbf{N}_{out} = \frac{\nabla S_{out}}{n_i}. \tag{3}$$

In general, the surface relief DOE locally transforms $\mathbf{N}_{inc}$ to $\mathbf{N}_{out}$ and has diffractive zones with gradually variable local orientation and grating period. Thus we can subdivide the DOE into small areas, each of which can be treated as a local surface relief diffraction grating characterized by its own parameters. In a DOE design, the goal is to find those grating parameters that provide the required change of beam propagation direction with high diffraction efficiency at each location $\mathbf{x}$ on the DOE. The local spatial frequency $\boldsymbol{\nu}$, grating period Λ, and grating orientation vector $\mathbf{s}$ are determined from the DOE equation,[2,8] which, in our notation and for the first diffraction order, yields

$$\boldsymbol{\nu} = \frac{1}{2\pi}\nabla_\perp\varphi = \frac{n_i}{\lambda}(\mathbf{N}_{out,\perp} - \mathbf{N}_{inc,\perp}), \tag{4}$$

$$\Lambda = \frac{1}{|\boldsymbol{\nu}|}, \quad \mathbf{s} = \frac{\boldsymbol{\nu}}{|\boldsymbol{\nu}|}, \quad |\mathbf{s}| = 1, \tag{5}$$

where $\nabla_\perp$ is the 2-D gradient operator with respect to lateral coordinates $\mathbf{x}$ along the DOE, $\mathbf{N}_{inc,\perp}$, $\mathbf{N}_{out,\perp}$ are the lateral components of the vectors $\mathbf{N}_{inc}$, $\mathbf{N}_{out}$, and φ is the DOE phase function, defined at each location $\mathbf{x}$ on the DOE as

$$\varphi = k(S_{out} - S_{inc}), \tag{6}$$

with $k = 2\pi/\lambda$.

When the eikonals S_{inc} and S_{out} satisfy geometrical optics restrictions, the phase function φ in Eq. (6) is naturally smooth and results in gradual zone distribution in the DOE. Equation (6) formally looks similar to that for a thin optical element[4] in the scalar domain. However, in the scalar domain, the phase function φ is independent of ray directions, while in other domains of light diffraction it does depend on the ray directions $\mathbf{N}_{inc}$, $\mathbf{N}_{out}$. When the incidence plane is perpendicular to the grating orientation vector $\mathbf{s}$, then the DOE Eq. (4) converts to a first-order grating equation in a classical mounting[8] as

$$n_i(\sin\theta_{inc} + \sin\theta_{out}) = \lambda/\Lambda. \tag{7}$$

In order to compare subwavelength, resonance, and scalar diffraction domains, we calculated the first-order diffraction efficiency of a sawtooth surface relief grating with a fixed depth but variable grating period. The results of the first-order TE diffraction efficiency as a function of the grating period, taken in units of wavelength, are presented in Fig. 2. These were calculated by a rigorous coupled wave approach[5] with the incidence angle 11.7°, $\lambda = 1\ \mu$m, $n_M = 1.4502$, and grating groove depth 2.17 μm which is optimal for obtaining highest diffraction efficiency in the scalar domain, in accordance with the equation[4]

$$\frac{h_{optScalar}}{\lambda} = \frac{1}{n_M - n_i}. \tag{8}$$

As evident, there are two ranges with nearly 100% diffraction efficiency. One is in the scalar diffraction domain, with grating periods larger than $\approx$17 illumination wavelengths. The other is in the resonance domain, with grating periods comparable with the illumination wavelength.

We found that in the scalar domain only the −1st diffraction order had high diffraction efficiency, whereas in the resonance domain it was the +1st diffraction order. The scalar domain suffers from higher diffraction orders accompanying the first diffraction order. The scalar domain is also restricted to low spatial frequency and small diffraction angles, leading to low numerical aperture (NA) of available diffractive lenses. The resonance domain in-

herently avoids disturbing higher diffraction orders, because they are evanescent. The zeroth and the −1st diffraction order in the resonance domain are well separated in direction from the main +1st diffraction order, because of the high diffraction angles occurring with the grating period comparable to the wavelength. Figure 2(a) shows the full range of grating periods and Fig. 2(b) shows a magnified part of the region around the resonance domain, both with a groove depth optimized for the scalar diffraction domain. Figure 3 shows a magnified part of the region around the resonance domain, but with groove depth 2.47 μm, which is optimal for obtaining highest diffraction efficiency in the resonance domain. Note that the diffraction efficiency in the resonance domain can reach 100%, even without any antireflection coating (Fig. 3), while the actual best diffraction efficiency in the scalar domain is ≈93% [Fig. 2(a)], where the reduction is due to diffraction losses into higher diffraction orders.

3. EFFECTIVE GRATING MODEL OF GRATINGS IN THE RESONANCE DOMAIN

Surface relief gratings in the resonance domain can be modeled with an effective grating model[18–20] by generalizing the effective medium theory[17] to include, in addition to the zeroth order, the first diffraction order. In this section we summarize the main features of the effective grating model and provide the relevant analytic closed-form equations for evaluating and designing DOEs in the resonance domain. For surface relief gratings in the resonance domain, where the grating period is comparable to that of the illumination wavelength, the diffraction efficiency of the first diffraction order can reach 100%, as shown in Fig. 3. Such unusually high diffraction efficiency for surface relief gratings was explained[18] by the two-wave Bragg diffraction phenomenon,[22] which is usually attributed only to volume hologram gratings. In the effec-

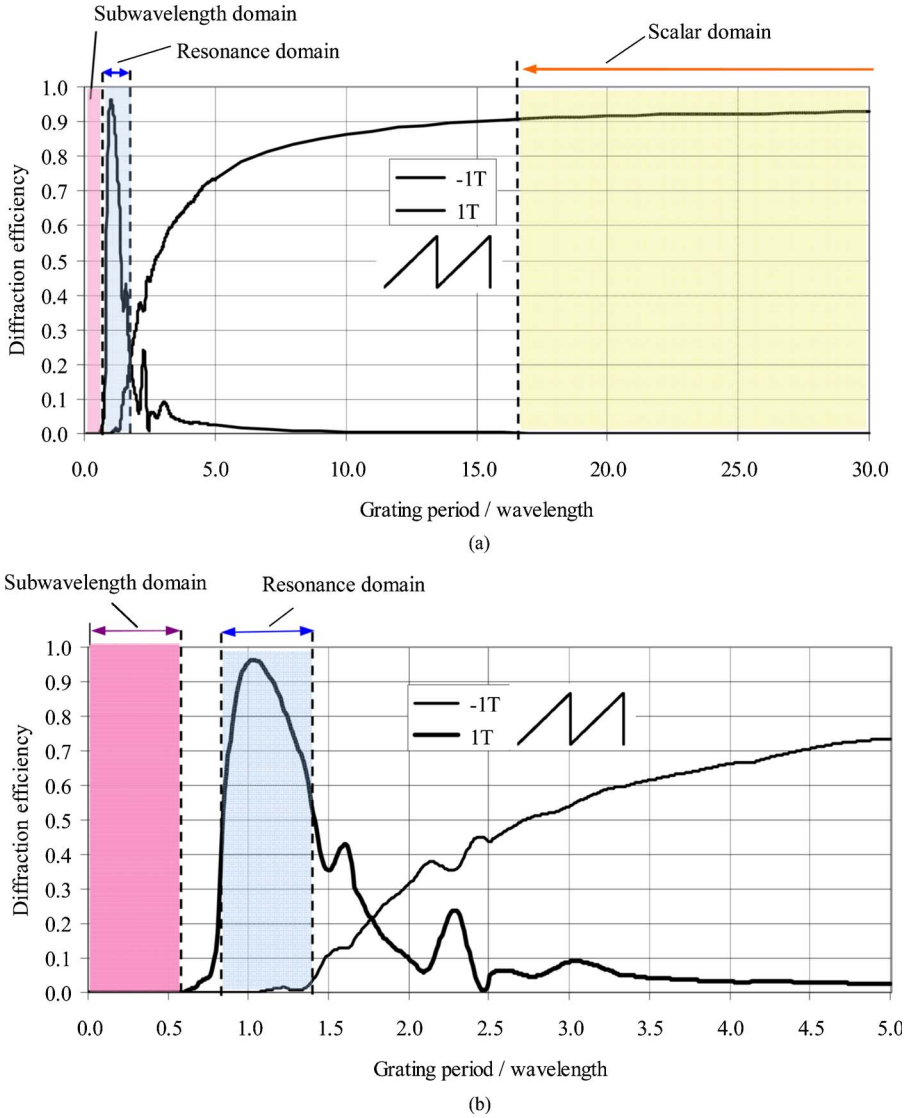

Fig. 2. (Color online) Diffraction efficiency as a function of grating period/wavelength when groove depth is optimized for the scalar domain, TE polarization. A diffraction order with highest diffraction efficiency is +1st for the resonance domain and −1st in the scalar domain. The graph is calculated by a rigorous coupled-wave analysis[5] for a sawtooth surface relief grating with incidence angle 11.7°, $\lambda = 1$ μm, $n_M = 1.45042$, and groove depth 2.17 μm. (a) Full range of grating periods, (b) magnified part showing mainly the resonance domain.

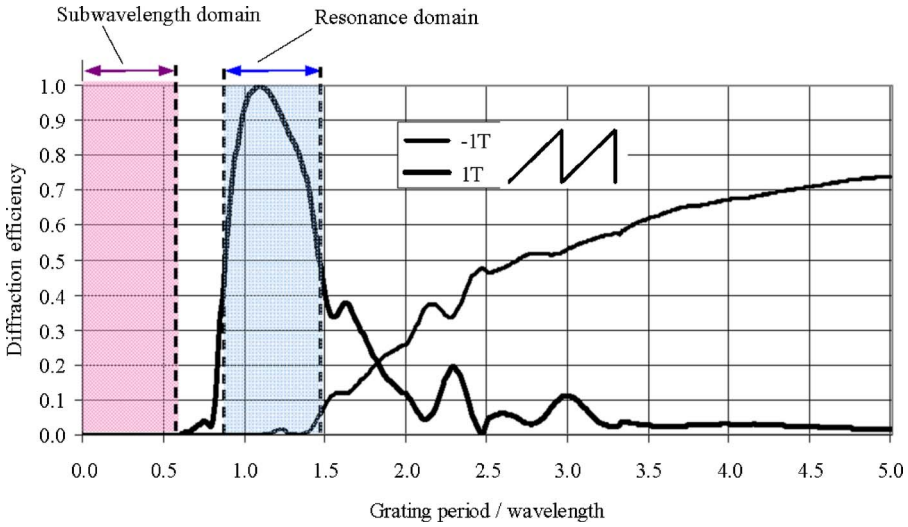

Fig. 3. (Color online) Diffraction efficiency as a function of grating period/wavelength when groove depth is optimized for the resonance domain, TE polarization. Magnified part showing mainly the resonance domain. The graph is calculated by a rigorous coupled-wave analysis (RCWA) for a sawtooth surface relief grating with incidence angle 11.7°, $\lambda=1\ \mu$m, $n_M=1.45042$, and groove depth 2.47 μm.

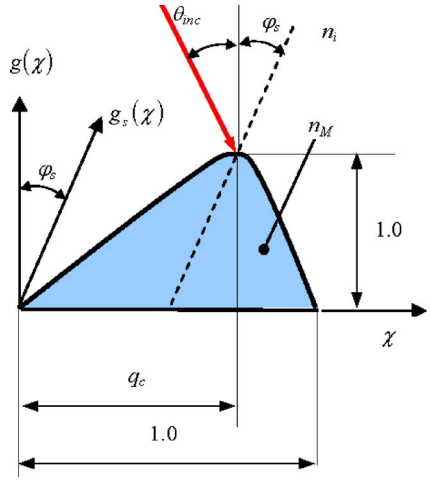

Fig. 4. (Color online) Geometric and optical parameters of a single groove of the surface relief grating.

tive grating model the profile of the surface relief grating groove is decomposed into sublayers. Light diffracted from these sublayers constructively interferes, resulting in the high Bragg diffraction efficiency.

The effective grating theory relates the high diffraction efficiency to the geometrical and optical parameters of the grooves in the surface relief gratings. For simplicity of the equations, a linear diffraction grating in classical mounting is assumed from this point. We begin with a general normalized groove profile defined by the function $g(\chi)$, $0 \le g(\chi) \le 1$, shown in Fig. 4. The groove profile is assumed unimodal and single-blazed and can have a variety of shapes, for instance, sinusoidal, rectangular, or triangular. As shown, χ is the normalized lateral coordinate ranging from 0 to 1 within the groove period Λ, q_c is the distance from the groove's edge to the center of the groove's peak, n_M and n_i are refractive indices of the groove material and surrounding medium, φ_s is the effective slant angle, and $g_s(\chi)$ is the normalized slanted groove profile.

The effective slant angle χ_s can be related to the groove's peak position[18] by

$$\tan \varphi_s = \frac{\Lambda}{h}(q_c - 0.5) = \frac{\Lambda}{h} p_s, \tag{9}$$

where effective slant parameter p_s is defined as $p_s = q_c - 0.5$ and h is the groove depth, which is actually the maximum value of the groove depth distribution $h \cdot g(\chi)$ within the period Λ. Using such a groove profile, the average refractive index $\bar{n}$ and the averaged first Fourier coefficient G_{1s} of the slanted groove profile were found to be

$$\bar{n}^2 = n_i^2 + \Delta n_M^2 \cdot \bar{g}, \tag{10}$$

$$G_{1s} = \int_0^1 g_s(\chi) \exp(-i 2\pi\chi) \mathrm{d}\chi, \tag{11}$$

with

$$\bar{g} = \int_0^1 g(\chi) \mathrm{d}\chi, \quad \Delta n_M^2 = n_M^2 - n_i^2. \tag{12}$$

The calculated G_{1s} for a triangular groove is $2/\pi^2 = 0.203$, and that for a sinusoidal groove is 0.25.[18,19]

The effective slant angle leads to an effective Bragg incidence angle $\theta_{inc,B}$, which may be related directly to parameters of the grooves by

$$n_i \sin \theta_{inc,B} = \frac{\lambda}{2\Lambda} - \tan \varphi_s \left[\frac{\bar{n}^2}{1 + \tan^2 \varphi_s} - \left(\frac{\lambda}{2\Lambda} \right)^2 \right]^{1/2} \tag{13}$$

and depends on the ratio Λ/λ, the effective slant angle φ_s, and the refractive indices via $\bar{n}$. At the Bragg incidence angle $\theta_{inc,B}$, the diffraction efficiency of the 1st diffraction order η_B is[18]

$$\eta_B = \sin^2\left(2\pi \frac{h}{\lambda} \frac{\bar{n}\bar{\kappa}_{01}}{\cos\varphi_s c_{0sB}}\right), \tag{14}$$

where

$$c_{0sB} = (1 - \sin^2\theta_{s1})^{1/2}, \quad \sin\theta_{s1} = \frac{\lambda}{2\bar{n}\Lambda\cos\varphi_s}, \tag{15}$$

and the coupling parameters $\bar{\kappa}_{01}$ in the cases of TE and TM polarizations are

$$\bar{\kappa}_{01TE} = \delta n_M^2 G_{1s}, \quad \delta n_M^2 = \frac{\Delta n_M^2}{2\bar{n}^2}, \tag{16}$$

$$\bar{\kappa}_{01TM} = \bar{\kappa}_{01TE}(1 - 2\sin^2\theta_{s1}). \tag{17}$$

Note that the resonance domain diffraction efficiency Eq. (14) substantially depends on Λ/λ, effective slant angle φ_s, the Fourier coefficient G_{1s} of the normalized groove profile, and also on the ration h/λ and refractive indices n_i, n_M. For comparison, a relative diffraction efficiency in the scalar domain depends only on h/λ and n_i, n_M, as[4]

$$\eta_{Scalar} = \mathrm{sinc}^2(h/h_{optScalar} - 1), \tag{18}$$

where $h_{optScalar}$ is determined from Eq. (8).

The effective grating model is based essentially based on the coupled wave theory of volume holograms with nearly Bragg incidence angle but is valid only in a specific period range $\Lambda_{low} < \Lambda < \Lambda_{up}$ of surface relief gratings.[18] A lower value Λ_{low} of the grating period is derived as $\Lambda_{low} = \max(\Lambda_{SW}, \Lambda_E)$, from two separate lower limits Λ_{SW} and Λ_E, which are both independent of the groove depth. An upper value Λ_{up} of the grating period is derived as $\Lambda_{up} = \min(\Lambda_B, \Lambda_A)$, from two separate upper limits Λ_B and Λ_A, with Λ_B independent of the groove depth.

The first lower limit Λ_{SW} is the grating period that defines the border between the subwavelength domain and the resonance domain. It is found from

$$\frac{\Lambda_{SW}}{\lambda} = \frac{1}{\min(\bar{n}, n_i) + n_i \sin\theta_{inc,B}}. \tag{19}$$

The second lower limit is the grating period that defines the border where the second-order derivatives in coupled wave equations[21] can be neglected. Accordingly, Λ_E must satisfy the equation

$$\bar{\kappa}_{01}/c_{0sB} = \gamma_{\max}, \tag{20}$$

with c_{0sB} and $\bar{\kappa}_{01}$ defined in Eqs. (15)–(17) and $\gamma_{\max} \approx 0.15$. The first upper limit Λ_B is the grating period that satisfies the two-wave Bragg diffraction regime criterion.[22] It is determined from

$$\frac{\Lambda_B}{\lambda} = \frac{\varepsilon_{high}^{1/4}}{\cos\varphi_s(\bar{n}\Delta n_s)^{1/2}}, \tag{21}$$

where $\Delta n_s = \Delta n_M^2 |G_{1s}|/\bar{n}$ is the refractive index modulation for the surface relief grating,[18] and ε_{high} estimates the power diffracted to other than the zeroth and first orders over the incidence beam power. In the development of the effective grating model the relative power ε_{high} was assumed to be zero, but a value of about 0.15 can be tolerated.

The second upper limit Λ_A is the grating period that defines for a certain aspect ratio h/Λ the border beyond which high Bragg diffraction efficiency cannot be obtained for the surface relief grating, even though it can be obtained for an effective volume grating. This is because the surface relief grating may include also additional gratings with slant parameters p as

$$p = p_s - \Delta p_{low} = \frac{h\tan\varphi_s}{\Lambda} - \Delta p_{low}, \tag{22}$$

where the calculated Δp_{low} for a triangular groove is 1.3524 and for a sinusoidal groove 1.052,[18,19] and p_s is the effective slant parameter of the effective grating [Eq. (9)]. To ensure that the light diffracted by the additional gratings is minimized, Λ_A should satisfy[18]

$$\bar{n}\left(Q_A - \tan\varphi_s\sqrt{\cos^2\varphi_s - Q_A^2}\right) = -\frac{\lambda}{2\Lambda_A} - \frac{\Lambda_A P}{h}\left[\frac{\bar{n}^2}{1 + (\Lambda_A p/h)^2} - \left(\frac{\lambda}{2\Lambda_A}\right)^2\right]^{1/2}, \tag{23}$$

where

$$Q_A = \frac{\lambda}{2\bar{n}\Lambda_A} - \frac{\xi_{mis}\cos^3\varphi_s}{\pi}\frac{\Lambda_A}{h}c_{0sB}, \quad \xi_{\mathrm{mis}} = 0.507. \tag{24}$$

To conclude, several limits and bounds must be imposed in order that the effective grating model of the surface relief grating in the resonance domain is valid. These include the following:

1. the groove profile should be unimodal and single-blazed;
2. the period Λ must be above lower limits Λ_{SW} and Λ_E, to exceed the subwavelength domain and satisfy coupled wave approximations;
3. the period Λ must be below upper limit Λ_B to have the two-wave Bragg diffraction;
4. the period Λ for a certain aspect ratio h/Λ must be below the upper limit Λ_A in order to minimize the influence of additional gratings. For typical optical materials, the range of periods $\Lambda_{low}, \Lambda_{up}$ is centered at about wavelength λ, compatible with the resonance domain gratings. To ensure that the DOEs are in the resonance domain, they must have small periods, comparable to λ, over their entire area. This is achieved with relatively high offset angles between the incident and output beams.

We verified our effective grating model in the resonance domain with the sawtooth surface relief grating where numerically derived diffraction efficiency as a function of grating period/wavelength is shown in Fig. 3. Specifically, we exploited the analytic effective grating Eqs. (14) and (13) to find the Bragg diffraction efficiency and the Bragg incidence angle at the grating period/wavelength of 1.1, where the peak of diffraction efficiency occurs. The results were calculated as Bragg diffraction efficiency of 99.90% and Bragg incidence angle of 11.74°. These are in a good agreement with the values of 99.70% and 11.7° that were obtained by rigorous numerical calculations.

4. ANALYTICAL DESIGN OF DIFFRACTIVE OPTICAL ELEMENTS IN THE RESONANCE DOMAIN

The relevant optical and geometrical parameters of the local surface relief gratings must be determined in order to obtain a DOE with desired local input and output beam directions and eikonals and with high diffraction efficiencies. These local parameters, such as the grating orientation vector **s**, period Λ, effective slant angle φ_s, relative peak position of groove q_c, groove depth h, and refractive index of groove material n_M can be determined analytically from our effective grating model and the DOE equations (4) and (5).

In order to obtain high (near 100%) diffraction efficiency η_B with given period Λ, the local grating must obey the Bragg condition of the equivalent grating model, Eq. (13). For the incidence angle θ_{inc} and a desired output diffraction angle θ_{out} such a Bragg condition will be satisfied if the groove effective slant angle φ_s is

$$\tan \varphi_s = \frac{\Lambda}{\lambda}[(\bar{n}^2 - n_i^2 \sin^2 \theta_{inc})^{1/2} - (\bar{n}^2 - n_i^2 \sin^2 \theta_{out})^{1/2}], \tag{25}$$

as derived from Eqs. (7) and (13). Then, substituting φ_s from Eq. (25) into Eq. (9) yields effective slant parameter p_s and relative groove peak position q_c as

$$P_s = \frac{h}{\Lambda} \tan \varphi_s, \quad q_c = 0.5 + p_s. \tag{26}$$

Now we are able to determine an optimal groove depth h_{opt} for a certain desired Bragg efficiency η_{Bd}. Since the functions c_{0rB} and $\bar{\kappa}_{01}$ depend only on Λ/λ and φ_s, we need to solve Eq. (14) in order to determine the groove depth h that would lead to this Bragg efficiency η_{Bd} at the Bragg incidence angle. For a specific value of η_{Bd}, there are two main solutions for the optimal groove depths for the TE polarization and two for the TM polarization, as

$$\frac{h_{opt}(\eta_{Bd})}{\lambda} = \frac{c_{0sB} \cos \varphi_s}{2\pi \bar{n} \bar{\kappa}_{01}} \left[\frac{\pi}{2} \pm \left(\frac{\pi}{2} - \arcsin \sqrt{\eta_{Bd}} \right) \right], \tag{27}$$

with $\bar{\kappa}_{01}$ for TE, $\bar{\kappa}_{01TE}$, and $\bar{\kappa}_{01}$ for TM, $\bar{\kappa}_{01TM}$, as in Eqs. (16) and (17). Note that any deviation of h from h_{opt} would lead to a change in the Bragg diffraction efficiency in accordance with Eq. (14). This is illustrated in Fig. 5, which shows the TE and TM Bragg diffraction efficiency as a function of the normalized groove depth h/λ. Also shown for comparison is the scalar domain diffraction efficiency, calculated in accordance with Eqs. (18) and (8). It is evident that the resonance domain diffraction efficiency of $\eta_{Bd} = 100\%$ for the TM polarization is achieved with larger optimal groove depth $h_{optTE}(\eta_{Bd})$ than that for the TE polarization $h_{optTE}(\eta_{Bd})$, whereby both of the TE and TM depths are larger than the prediction of the scalar domain diffraction for an optimal groove depth $h_{optScalar}$[Eq. (8)].

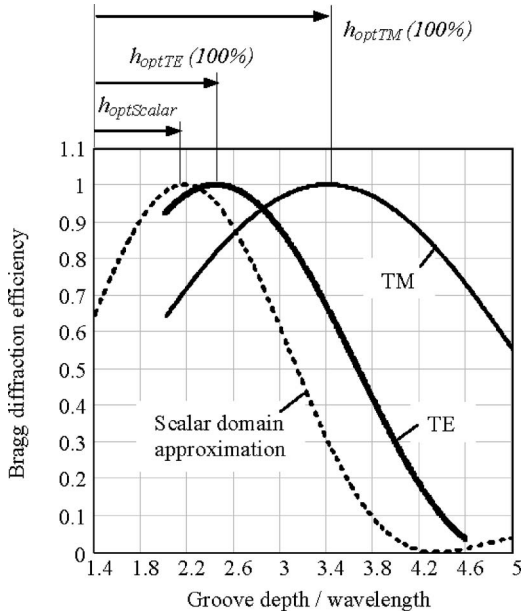

Fig. 5. Bragg TE and TM diffraction efficiency for surface relief gratings with triangular groove profiles as functions of the normalized groove depth h/λ for the resonance domain and for the scalar domain. Calculations were done by the effective grating model. Effective slant angle is $\varphi_s = 15°$, $\Lambda/\lambda = 1.1$, refractive index of grooves $n_M = 1.46$, $n_i = 1$.

To illustrate our analytic design of DOEs in the resonance domain, we consider a cylindrical focusing diffractive lens having a desired high diffraction efficiency of η_{Bd}. In order to keep the DOE grating periods within the bounds $\Lambda_{low} < \Lambda < \Lambda_{up}$ and comparable to the illumination wavelength λ, we need relatively high off-axis angles. The geometrical parameters of the lens are depicted in Fig. 6. Figure 6(a) shows the entire geometry of the lens and Fig. 6(b) a magnified one-dimensional cross section. As shown the grating grooves are oriented parallel to the y axis.

The phase function of the cylindrical focusing diffractive lens, which transforms an oblique plane incident wave to an off-axis converging cylindrical wave is

$$\varphi(x) = \frac{2\pi}{\lambda}\{F[1 - \gamma(x)] - x \sin \theta_{inc}\}, \tag{28}$$

where $|x| < D/2$, D is the lens aperture, α is the off-axis angle of the converging cylindrical lens, F is the focal length, θ_{inc} is the incidence angle of the incident plane wave, the same for all locations x on the lens, and

$$\gamma(x) = \sqrt{1 + 2 \sin \alpha \frac{x}{F} + \frac{x^2}{F^2}}. \tag{29}$$

Note that when $D \ll F$, $\varphi(x)$ of Eq. (28) can be approximated by

$$\varphi(x) \equiv \frac{2\pi}{\lambda}\left\{ - (\sin \theta_{inc} + \sin \alpha)x - \frac{x^2}{2F} \right\}. \tag{30}$$

The spatial frequency and local grating period in accordance with the DOE Eqs. (4) and (5), are

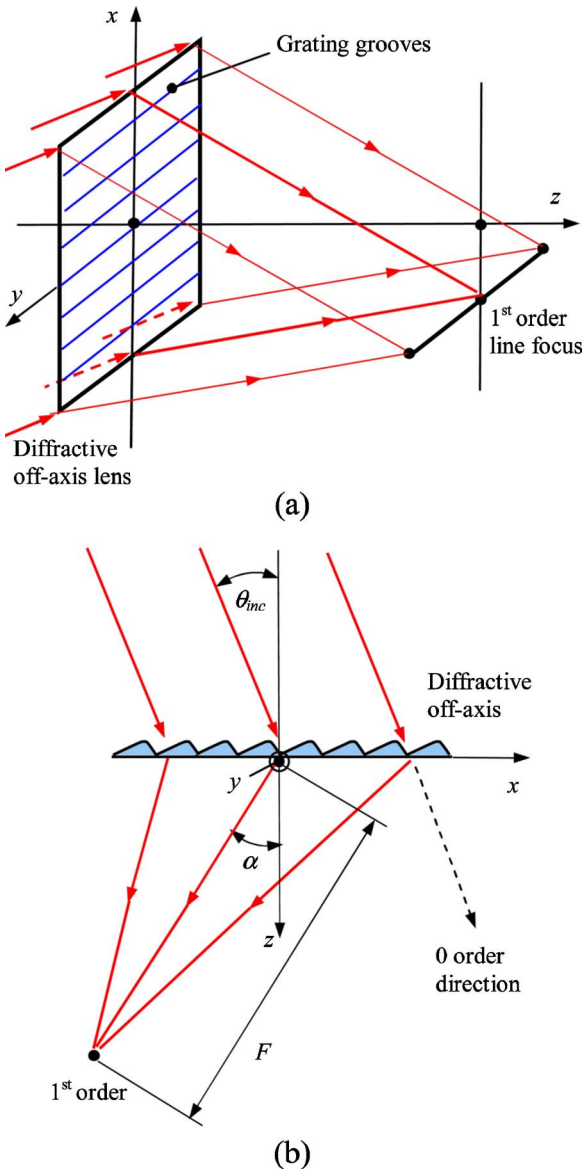

Fig. 6. (Color online) Geometrical parameters of the off-axis one-dimensional focusing diffractive lens. (a) entire lens, (b) magnified one-dimensional cross section.

$$\nu_x = -\frac{1}{\lambda}[\sin\theta_{inc} + \sin\theta_{out}], \tag{31}$$

$$\Lambda = \frac{1}{|\nu_x|}, \tag{32}$$

where

$$\sin\theta_{out} = \frac{\sin\alpha + x/F}{\gamma(x)}. \tag{33}$$

Then, the effective local slant angle φ_s is determined from Eq. (25), the groove peak position q_c from Eqs. (26), and the groove depth h from Eq. (27).

We designed a specific diffractive cylindrical lens in the resonance domain using the following parameters: $\lambda = 0.633$ mm, $n_M = 1.457$, $n_i = 1$, $\alpha = 45°$, $\theta_{inc} = 15°$, $F = 50$ mm, $D = 25$ mm, $\eta_{Bd} = 100\%$ and triangular groove profiles. Specifically, we calculated the local normalized grating periods, effective slant angles, groove peak positions, and the groove depths, all as a function of relative lateral coordinates $2x/D$ of the diffractive lens. The results are presented in Figs. 7–10 and in Table 1. Figure 7 shows the variations of the grating period Λ normalized with respect to the wavelength, as well as its lower and upper period bounds Λ_{low} and Λ_{up}. As is evident, the actual normalized periods Λ/λ range from 1.25 to 0.94, so they fall within these bounds.

Figures 8 and 9 depict variations of the local effective slant angle and groove peak position that satisfy the Bragg condition locally at each coordinate x of the diffractive cylindrical lens. Figures 8 and 9 indicate that at the

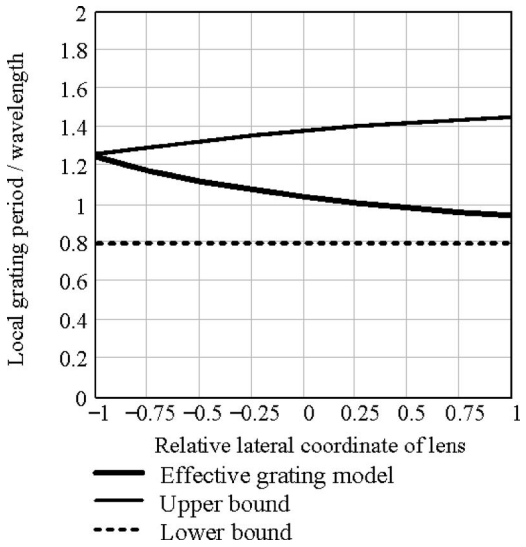

Fig. 7. Variations of the normalized local grating period Λ/λ of the diffractive off-axis cylindrical lens in the resonance domain as a function of the relative lateral coordinate $2x/D$ on the lens. Also shown are the lower and upper period bounds Λ_{low} and Λ_{up}. Parameters are $\lambda = 0.633$ mm, $n_M = 1.457$, $\alpha = 45°$, $\theta_{inc} = 15°$, $F = 50$ mm, $D = 25$ mm, $\eta_{Bd} = 100\%$.

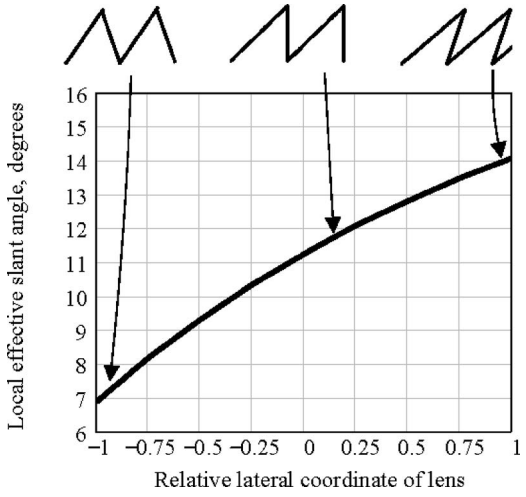

Fig. 8. Variations of the local effective slant angle φ_s of the resonance domain diffractive off-axis cylindrical lens, which provide the Bragg condition locally at each coordinate x point of the cylindrical lens, plotted as a function of the relative lateral coordinate $2x/D$ on the lens. Parameters are the same as in Fig. 7.

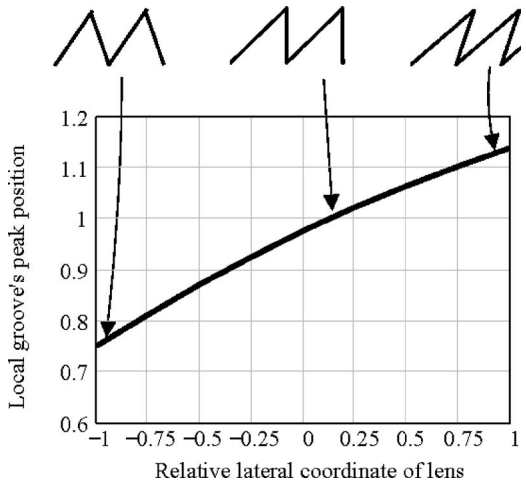

Fig. 9. Variations of the relative groove peak position q_c of the resonance domain diffractive off-axis cylindrical lens, which provide Bragg condition locally at each coordinate x point of the cylindrical lens, plotted as a function of the relative lateral coordinate $2x/D$ on the lens. Parameters are the same as in Fig. 7.

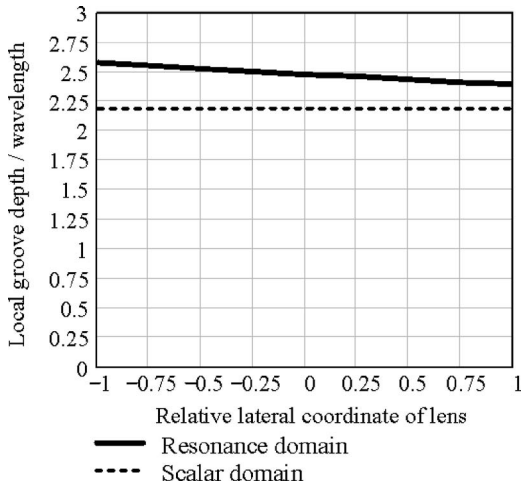

Fig. 10. Variations of the required normalized local groove depths $h_{opt}(\eta_{Bd})/\lambda$ of the resonance domain diffractive off-axis cylindrical lens, which provide the Bragg condition with $\eta_{Bd}=100\%$ locally at each coordinate x point of the cylindrical lens, plotted as a function of the relative lateral coordinate $2x/D$ on the lens. Also shown is the scalar depth $h_{optScalar}$. Parameters are $\lambda=0.633$ mm, $n_M=1.457$, $\alpha=45°$, $\theta_{inc}=15°$, $F=50$ mm, $D=25$ mm.

edge of the lens, −1 relative lateral coordinate, the grating grooves have a nearly symmetrical shape ($\varphi_s=6.9°$, $q_c=0.75$, compared with $q_c=0.5$ of a symmetrical groove). At about the center of the lens, 0.13 relative lateral coordinate, the grooves have a sawtooth shape ($\varphi_s=11.7°$, $q_c=1.0$). Finally, at the other edge of the lens, +1 relative lateral coordinate, the grooves have a significant "overhang" ($\varphi_s=14.1°$, $q_c=1.14$) whereby one grating period overlaps the adjacent one.

Figure 10 depicts variations of the required normalized local groove depths $h_{opt}(\eta_{Bd})/\lambda$ which provide $\eta_{Bd}=100\%$ locally at each coordinate x of the diffractive cylindrical lens. Also shown are the calculated results for the scalar domain groove depth $h_{optScalar}/\lambda$. It is again evident that the resonance domain requires slightly deeper grooves than the scalar domain. We verified that these grating periods, effective slant angles, groove peak positions, and the groove depths, which were calculated by our effective grating model, indeed result in high diffraction efficiencies. For this we calculated the diffraction efficiency of the first order by numerical (RCWA)[5] and got 96.9% at the edge of the lens, −1 relative lateral coordinate; 99.7% at about the center of lens, 0.13 relative lateral coordinate; and 99.8% at the other edge of the lens, +1 relative lateral coordinate that is in agreement with desired value of $\eta_{Bd}=100\%$. Table 1 summarizes all the results of Figs. 7–10, showing the relevant parameters obtained with one design at these local grating locations.

For all the results in this illustration example, the basic shape of the slanted grooves could be sinusoidal, rectangular, or triangular. Such a variety of shapes is possible because diffraction efficiency depends on the first Fourier coefficient G_{1s} of a groove profile, rather than on the details of the profile. It is only necessary that the groove profiles have the proper effective slant angles and aspect ratios, as well as the proper local grating periods that do fit the actual G_{1s} value.

5. CONCLUDING REMARKS

We developed and investigated a model for designing and analyzing resonance domain surface relief DOEs. It is based on transforming the surface relief modulation to an effective grating with slanted volume fringes that can provide closed-form analytical solutions. The local period

Table 1. Design Data for the Local Diffraction Gratings of the Resonance Domain Off-Axis One-Dimensional Focusing Diffractive Lens[a]

Position on the Lens	Edge	Center	Other Edge
Relative lateral coordinate on the lens	−1	+0.13	+1
Local grating period/wavelength	1.25	1.02	0.94
Local groove depths/wavelength	2.58	2.46	2.39
Scalar groove depth/wavelength	—	2.19	—
Local effective slant angle	6.9°	11.7°	14.1°
Local relative groove-peak position	0.75	1.0	1.14
Groove shape	Nearly symmetrical	Sawtooth	Overhanging
Groove scheme	See Figs. 8 and 9	See Figs. 8 and 9	See Figs. 8 and 9
Diffraction efficiency, RCWA	96.9%	99.7%	99.8%
Diffraction efficiency designed		100%	

[a]Given parameters are $\lambda=0.633$ mm, $n_M=1.457$, $\alpha=45°$, $\theta_{inc}=15°$, $F=50$ mm, $D=25$ mm.

of the DOE, angular orientation of diffractive zones, and effective slant angle are chosen to ensure required transformation of the local incident beam angular direction to the desired output beam angular direction and satisfy the local Bragg condition. The groove depths are optimized for achieving nearly 100% Bragg diffraction efficiency. We determined a specific grating period range of $\Lambda_{low} < \Lambda < \Lambda_{up}$ within the resonance domain where the effective grating model is applicable. Both bounds depend on refractive indices, and the upper bound depends also on the ratio of the groove depth to the grating period. Thus, the design and analysis of the complicated resonance domain DOEs with wavelength-scale features can now be performed with almost the same simplicity as that of well-known scalar domain design and analysis.

ACKNOWLEDGMENT

The work reported in this paper was started while Michael Golub was at the Department of Physics of Complex Systems, Weizmann Institute of Science, Rehovot, Israel.

Michael Golub can be reached by e-mail at mgolub@eng.tau.ac.il.

REFERENCES

1. L. B. Lesem, P. M. Hirsch, and J. A. Jordan, "The kinoform: a new wavefront reconstruction device," IBM J. Res. Dev. **13**, 150–155 (1969).
2. E. Hasman and A. A. Friesem, "Analytic optimization for holographic optical elements," J. Opt. Soc. Am. A **6**, 62–72 (1989).
3. M. A. Golub, I. N. Sissakian, and V. A. Soifer, "Infra-red radiation focusators," Opt. Lasers Eng. **15**, 297–309 (1991).
4. M. A. Golub, "Generalized conversion from the phase function to the blazed surface-relief profile of diffractive optical elements," J. Opt. Soc. Am. A **16**, 1194–1201 (1999).
5. M. G. Moharam and T. K. Gaylord, "Diffraction analysis of dielectric surface-relief gratings," J. Opt. Soc. Am. **72**, 1385–1392 (1982).
6. S. Peng and G. M. Morris, "Efficient implementation of rigorous coupled-wave analysis for surface-relief gratings," J. Opt. Soc. Am. A **12**, 1087–1096 (1995).
7. L. Li, J. Chandezon, G. Granet, and J.-P. Plumey, "Rigorous and efficient grating-analysis method made easy for optical engineers," Appl. Opt. **38**, 304–313 (1999).
8. M. Nevière and E. Popov, *Light Propagation in Periodic Media* (Marcel Dekker, 2003).
9. M. L. Lee, P. Lalanne, J. Rodier, and E. Cambril, "Wide field-angle behavior of blazed-binary gratings in the resonance domain," Opt. Lett. **25**, 1690–1692 (2000).
10. Y. Sheng, D. Feng, and S. Larochelle, "Analysis and synthesis of circular diffractive lens with local linear grating model and rigorous coupled-wave theory," J. Opt. Soc. Am. A **14**, 1562–1568 (1997).
11. S. Shi and D. W. Prather, "Electromagnetic analysis of axially symmetric diffractive optical elements illuminated by oblique incident plane waves," J. Opt. Soc. Am. A **18**, 2901–2907 (2001).
12. T. Shiono, T. Hamamoto, and K. Takahara, "High-efficiency blazed diffractive optical elements for the violet wavelength fabricated by electron-beam lithography," Appl. Opt. **41**, 2390–2393 (2002).
13. E. Noponen, A. Vasara, J. Turunen, J. M. Miller, and M. R. Taghizadeh, "Synthetic diffractive optics in the resonance domain," J. Opt. Soc. Am. A **9**, 1206–1213 (1992).
14. A. Schilling and H. P. Herzig, "Phase function encoding of diffractive structures," Appl. Opt. **39**, 5273–5279 (2000).
15. J. M. Miller, N. Beaucoudrey, P. Chavel, J. Turunen, and Edmond Cambril, "Design and fabrication of binary slanted surface-relief gratings for a planar optical interconnection," Appl. Opt. **36**, 5717–5727 (1997).
16. T. Vallius, J. Tervo, P. Vahimaa, and J. Turunen, "Electromagnetic field computation in semiconductor laser resonators," J. Opt. Soc. Am. A **23**, 906–911 (2006).
17. D. H. Raguin and G. M. Morris, "Antireflection structured surfaces for the infrared spectral region," Appl. Opt. **32**, 1154–1167 (1993).
18. M. A. Golub and A. A. Friesem, "Effective grating theory for the resonance domain surface relief diffraction gratings," J. Opt. Soc. Am. A **22**, 1115–1126 (2005).
19. M. A. Golub, A. A. Friesem, and L. Eisen, "Bragg properties of efficient surface relief gratings in the resonance domain," Opt. Commun. **235**, 261–267 (2004).
20. M. A. Golub and A. A. Friesem, "Analytical theory for efficient surface relief gratings in the resonance domain," in *The Art and Science of Holography: A Tribute to Emmett Leith and Yuri Denisyuk*, H. John Caulfield, ed. (SPIE Press, 2004) Chap. 19, pp. 307–328.
21. H. Kogelnik, "Coupled wave theory for thick hologram gratings," Bell Syst. Tech. J. **48**, 2909–2947 (1969).
22. M. G. Moharam, T. K. Gaylord, and R. Magnusson, "Criteria for Bragg regime diffraction by phase gratings," Opt. Commun. **32**, 14–18 (1980).